

Classical scale-invariance, the electroweak scale and vector dark matter

Christopher D. Carone* and Raymundo Ramos†

*High Energy Theory Group, Department of Physics,
College of William and Mary, Williamsburg, VA 23187-8795*

(Dated: July 2013)

Abstract

We consider a classically scale-invariant extension of the standard model in which a dark, non-Abelian gauge symmetry is spontaneously broken via the Coleman-Weinberg mechanism. Higgs portal couplings between the dark and standard model sectors provide an origin for the Higgs mass squared parameter and, hence, the electroweak scale. We find that choices for model parameters exist in which the dark gauge multiplet is viable as dark matter.

*cdcaro@wm.edu

†raramos@email.wm.edu

I. INTRODUCTION

Over the past decade, solutions to the hierarchy problem have been dominated by an appealing theoretical paradigm: partners to standard model particles are postulated to cancel the quadratic divergence that otherwise affects the Higgs boson squared mass. These partners can have spins that differ from those of their standard model counterparts, as in the minimal supersymmetric standard model (MSSM) [1], or the same spins, as in little Higgs models [2]. They can be associated with states in Hilbert space of positive norm, as in the preceding two examples, or states of negative norm, as in the Lee-Wick standard model [3]. A point of commonality in all these scenarios is the requirement that the partner particles appear at or near the electroweak scale, which one might reasonably identify with the Higgs field vacuum expectation value (vev), $v = 246$ GeV. Searches at the Large Hadron Collider (LHC) for new particles around this energy scale have, aside from the Higgs boson, produced null results [4].

Of course, all the scenarios described in the preceding paragraph have a decoupling limit, and it is a matter of taste how much fine-tuning one is willing to tolerate before concluding that a given proposal is disfavored. One might hope that the planned energy upgrade at the LHC will provide more definitive results. Nevertheless, the absence of even small indirect effects of partner particles in the current LHC data motivates the study of alternative paradigms. Here, we consider a scenario first discussed by Bardeen [5], and studied recently by many others [6–10], that the standard model may possess a softly-broken classical scale-invariance that protects it from unwanted quadratic divergences. Such a scenario can be realized if the standard model Lagrangian has no dimensionful parameters and the Higgs mass arises via dimensional transmutation. This can occur if the Higgs field couples to a new strongly interacting sector, as explored in Refs. [11]. (For a much earlier example of a classically scale-invariant theory in which the Higgs boson mass is determined via dimensional transmutation in a strongly interacting sector, see Ref. [12].) Alternatively, the Higgs boson mass can arise in a classically scale-invariant theory that is weakly coupled via the Coleman-Weinberg (CW) mechanism [13]. It is well known that the CW mechanism applied to the standard model alone leads to a Higgs boson mass that is much smaller than the electroweak gauge boson masses, and hence is not viable. However, Refs. [6–8] demonstrate explicitly that modest extensions of the standard model can avoid this problem.

It is this general approach that we pursue in the model building discussed in this paper.

The argument of Bardeen has been rephrased a number of times in Refs. [7, 8], with additional justification and emphasis varying from paper to paper (See also a summary given in a talk by Lykken [14]). Rather than repeating this discussion, we refer the reader to these references; here make only a few comments. In order for an extension of the standard model to be classically scale invariant and free of quadratic divergences, one first assumes that the tree-level Higgs mass term is absent and that there are no higher mass scales associated with new heavy particle thresholds, as would be the case, for example, in a grand unified theory. The latter requirement precludes a conventional see-saw mechanism for the generation of small neutrino masses, so we will simply assume that neutrinos have Dirac mass terms with small Yukawa couplings. As in the charged fermion sector, small neutrino masses are then technically natural [15] since chiral symmetries are restored in the limit of vanishing Yukawa couplings. As flavor physics is not the focus of the present work, this assumption will suffice for the present purposes. If one then works with a regulator that does the least violence to the classical symmetry (namely, dimensional regularization), then one observes that a Higgs mass squared generated radiatively in the infrared is only multiplicatively renormalized [8]; this indicates that it too is technically natural. The only remaining assumption is that quantum gravitational physics does not spoil this outcome even though it is associated with a dimensionful scale, *viz.*, the Planck scale $M_{Pl} = 1.22 \times 10^{19}$ GeV (or alternatively, the reduced Planck scale, $M_* = 2.43 \times 10^{18}$ GeV). Our current uncertainty about the nature of quantum gravity makes this at most a plausible working assumption, but one that leads to a relatively restrictive framework for low-energy model building. Such models can be more readily put to direct experimental tests.

The model we study is one in which the standard model is extended by an additional $SU(2)_D$ gauge group and a complex scalar doublet Φ that transforms only under this new gauge symmetry. The subscript represents the word “dark”, since the new gauge sector only communicates with the standard model via a coupling between Φ and the standard model Higgs doublet field H ,

$$\lambda_p \Phi^\dagger \Phi H^\dagger H \ , \tag{1.1}$$

where λ_p is typically small. This is the well-known Higgs portal, one of the small number of possible renormalizable couplings between standard model fields and a new sector of particles that are singlets under the standard model gauge group. In the present case, the

dark sector is scale invariant at tree level and undergoes spontaneous symmetry breaking via the Coleman-Weinberg mechanism. Hence, the vev $\langle\Phi\rangle \equiv v_D/\sqrt{2}$, which provides an origin for the Higgs boson mass scale via Eq. (1.1), is determined by dimensional transmutation. The $SU(2)_D$ gauge group is spontaneously broken, leading to a degenerate triplet of massive gauge bosons A^a , $a = 1 \dots 3$, with masses $m_A \equiv g_D v_D/2$, where g_D is the $SU(2)_D$ gauge coupling. These spin-one states are stable and are potential dark matter candidates. One of the results we present in this paper is that there are parameter choices consistent with viable Coleman-Weinberg symmetry breaking as well as the correct relic density of the $SU(2)_D$ gauge multiplet.

The motivation for the work we present on this model can also be framed in the context of the existing related literature. Let us give three different rationales that may appeal to readers with different theoretical tastes:

i.) The use of the Higgs portal as a means for communicating Coleman-Weinberg symmetry breaking in a dark sector to the standard model has been discussed recently in the context of Abelian dark gauge groups in Refs. [8]. Our work considers the phenomenology in a model based on a non-Abelian dark gauge group, a natural alternative possibility.

ii.) The possibility that dark matter may be spin-one is well known, and the case in which the dark matter is a massive $SU(2)$ gauge multiplet has been considered in Refs. [16]. In this scenario, called Hidden Vector Dark Matter, the doublet field Φ together with the H are assumed to have the most general scalar potential. Our work studies the Coleman-Weinberg limit of the potential, leading to a model that is parametrically simpler and whose phenomenology is more constrained.

iii.) There has been interest in dark matter models in which the dark matter candidate can annihilate predominantly into lighter, unstable intermediate particles. These “secluded dark matter” scenarios [17] are less constrained by direct dark matter searches, since the annihilation cross section and the dark matter-nucleon elastic scattering cross section are determined by different combinations of couplings. Our work studies a simple model that falls into this interesting category.

Our paper is organized as follows. In Sec. II, we define the model and our conventions. In Sec. III, we consider phenomenological constraints on the model, including vacuum stability, perturbativity, and some aspects of Higgs boson physics. In Sec. IV, we consider the parameter ranges in which the model can provide a viable vector dark matter candidate. In

Sec. V, we summarize our conclusions.

II. THE MODEL

The gauge symmetry of the model is $G_{\text{SM}} \times \text{SU}(2)_D$, where G_{SM} is the standard model gauge group. The standard model particle content is assumed to include three right-handed neutrinos so that neutrino Dirac masses are possible, for the reasons described in the introduction. In addition, the model includes a complex scalar doublet under $\text{SU}(2)_D$. No fermions transforming under the dark gauge group are present, so the model is free of gauge anomalies.

At tree-level, the scalar potential is given by

$$V(\Phi, H) = \frac{1}{2}\lambda(\Phi^\dagger\Phi)^2 - \lambda_p(H^\dagger H)(\Phi^\dagger\Phi) + \frac{1}{2}\lambda_H(H^\dagger H)^2, \quad (2.1)$$

where H is the standard model Higgs doublet field. Mass terms for the Φ and H fields are omitted, in accordance with the assumption of classical scale invariance. Note that Eq. (2.1) can be rewritten

$$V(\Phi, H) = \frac{1}{2}\lambda_H \left(H^\dagger H - \frac{\lambda_p}{\lambda_H} \Phi^\dagger\Phi \right)^2 + \frac{1}{2} \left(\lambda - \frac{\lambda_p^2}{\lambda_H} \right) (\Phi^\dagger\Phi)^2, \quad (2.2)$$

from which one can read off the tree-level vacuum stability conditions

$$\lambda_H > 0 \quad \text{and} \quad \lambda \lambda_H > \lambda_p^2. \quad (2.3)$$

We will refer to these conditions again later in our analysis.

Given the absence of dimensionful couplings, it is not surprising that minimization of Eq. (2.1) gives $\langle\Phi\rangle = \langle H\rangle = 0$. This outcome, however, does not persist when quantum corrections to $V(\Phi, H)$ are taken into account [13]. We include the one-loop contributions to the effective potential that involve the $\text{SU}(2)_D$ gauge bosons and the top quark. For the numerical values of the couplings that are relevant in our later analysis, these represent the leading corrections. Defining the classical fields ϕ and σ by

$$\Phi = \frac{1}{\sqrt{2}} \begin{pmatrix} 0 \\ \phi \end{pmatrix} \quad \text{and} \quad H = \frac{1}{\sqrt{2}} \begin{pmatrix} 0 \\ \sigma \end{pmatrix}, \quad (2.4)$$

the one-loop effective potential may be written

$$V(\phi, \sigma)^{\overline{\text{MS}}} = \frac{1}{8}\lambda\phi^4 + \frac{9}{1024\pi^2}g_D^4\phi^4 \left(\ln \frac{g_D^2\phi^2}{4\mu^2} - \frac{3}{2} \right) - \frac{1}{4}\lambda_p\sigma^2\phi^2 \\ + \frac{1}{8}\lambda_H\sigma^4 - \frac{3}{64\pi^2}h_t^4\sigma^4 \left(\ln \frac{h_t^2\sigma^2}{2\mu^2} - \frac{3}{2} \right) , \quad (2.5)$$

where h_t is the top quark Yukawa coupling. In Eq. (2.5) we work in the $\overline{\text{MS}}$ scheme and μ is the renormalization scale. We extremize the potential by evaluating

$$\frac{\partial V}{\partial \phi} = \frac{\partial V}{\partial \sigma} = 0 , \quad (2.6)$$

with V and the couplings contained therein evaluated at the renormalization scale $\mu = \langle \sigma \rangle \equiv v$. (Note that we use this potential only to relate couplings defined at the electroweak scale and vevs that do not differ wildly from the same scale. For this purpose, renormalization group improvement is not necessary to achieve reliable results.) This leads to two constraints on the solution with nonvanishing $\langle \phi \rangle$ and $\langle \sigma \rangle$,

$$\lambda_H = \lambda_p \frac{\langle \phi \rangle^2}{\langle \sigma \rangle^2} - \frac{3}{8\pi^2}h_t^4 \left[1 - \ln \left(\frac{h_t^2}{2} \right) \right] , \quad (2.7)$$

$$\lambda = \frac{9}{128\pi^2}g_D^4 \left[1 - \ln \left(\frac{g_D^2\langle \phi \rangle^2}{4\langle \sigma \rangle^2} \right) \right] + \lambda_p \frac{\langle \sigma \rangle^2}{\langle \phi \rangle^2} . \quad (2.8)$$

We fix $\langle \sigma \rangle \equiv v = 246$ GeV, as indicated earlier, while $h_t = \sqrt{2}m_t/v$ follows numerically from the $\overline{\text{MS}}$ value of the top quark mass, $m_t = 160_{-4}^{+5}$ GeV [18]. Thus far, Eqs. (2.7) and (2.8) imply that one can take the free parameters of the model to be g_D , λ_p and $\langle \phi \rangle$.

We know, however, that one parametric degree of freedom is fixed by the requirement that one of the two scalar mass eigenstates must correspond to the Higgs boson observed at the LHC. To proceed, we consider the scalar mass squared matrix that follows from Eqs. (2.5), (2.7) and (2.8):

$$M^2 = \begin{bmatrix} \langle \phi \rangle^2 \lambda_p + \Delta m^2 & -\lambda_p \langle \sigma \rangle \langle \phi \rangle \\ -\lambda_p \langle \sigma \rangle \langle \phi \rangle & \frac{9}{128\pi^2}g_D^4 \langle \phi \rangle^2 + \lambda_p \langle \sigma \rangle^2 \end{bmatrix} . \quad (2.9)$$

Here, $\Delta m^2 = -3h_t^4\langle \sigma \rangle^2/(8\pi^2)$ is the shift in the Higgs boson mass in the standard model due to the top quark loop correction. For given input values of (g_D, λ_p) , we solve for $\langle \phi \rangle$ numerically by identifying either eigenvalue of Eq. (2.9) with the Higgs boson mass $m_h = 125$ GeV. The two choices correspond to either $m_\eta > m_h$ or $m_\eta < m_h$, where we let η represent the other scalar mass eigenstate. We define the mixing angle θ by

$$\begin{pmatrix} \cos \theta & -\sin \theta \\ \sin \theta & \cos \theta \end{pmatrix} \begin{pmatrix} h \\ \eta \end{pmatrix} = \begin{pmatrix} \sigma_0 \\ \varphi \end{pmatrix} , \quad (2.10)$$

where φ and σ_0 are the physical fluctuations about the vevs: $\phi = \langle \phi \rangle + \varphi$ and $\sigma = \langle \sigma \rangle + \sigma_0$. It follows that $\tan 2\theta = 2M_{12}^2/(M_{11}^2 - M_{22}^2)$, where M_{ij}^2 are the elements of the matrix in Eq. (2.9).

The phenomenology of the model may now be specified in terms of a two-dimensional parameter space, the (g_D, λ_p) plane. We begin isolating interesting regions of this parameter space in the next section.

III. PHENOMENOLOGICAL CONSTRAINTS

Given our assumption that there are no new, physical mass scales between the weak and Planck scales, we first require that viable points in parameter space do not lead to Landau poles below M_* in any of the couplings. This precludes the possibility that a Landau pole is a symptom of omitted new physics that is associated with an intermediate mass scale. Of course, before a Landau pole is reached, a given coupling will become nonperturbatively large, and one cannot be sure that it actually blows up. We simply impose the requirement that λ , λ_H and λ_p remain each smaller than 3 below $\mu = M_*$. We find that the allowed parameter space of the model is not significantly enlarged for larger choices of this numerical limit, since couplings that exceed it tend to do so very quickly. To proceed, we numerically evaluate the following one-loop renormalization group equations (RGEs),

$$16\pi^2 \frac{d\lambda}{dt} = 12\lambda^2 + 4\lambda_p^2 - 9g_D^2\lambda + \frac{9}{4}g_D^4, \quad (3.1)$$

$$\begin{aligned} 16\pi^2 \frac{d\lambda_H}{dt} = & 12\lambda_H^2 + 4\lambda_p^2 + \frac{9}{4} \left(\frac{3}{25}g_1^4 + \frac{2}{5}g_1^2g_2^2 + g_2^4 \right) \\ & - \left(\frac{9}{5}g_1^2 + 9g_2^2 \right) \lambda_H + 12h_t^2\lambda_H - 12h_t^4, \end{aligned} \quad (3.2)$$

$$16\pi^2 \frac{d\lambda_p}{dt} = \lambda_p \left(6\lambda - 4\lambda_p + 6\lambda_H + 6h_t^2 - \frac{9}{2}g_2^2 - \frac{9}{10}g_1^2 - \frac{9}{2}g_D^2 \right), \quad (3.3)$$

$$16\pi^2 \frac{dg_D}{dt} = -\frac{43}{6}g_D^3. \quad (3.4)$$

Here h_t , g_1 , g_2 and g_3 are evolved according to the one-loop standard model RGEs

$$16\pi^2 \frac{dh_t}{dt} = \left[-\frac{17}{20}g_1^2 - \frac{9}{4}g_2^2 - 8g_3^2 + \frac{9}{2}h_t^2 \right] h_t, \quad (3.5)$$

$$16\pi^2 \frac{dg_i}{dt} = b_i g_i^3, \quad (3.6)$$

where $b_i = (\frac{41}{10}, -\frac{19}{6}, -7)$ and we use the SU(5) normalization of hypercharge. In addition to the assignment of initial conditions described in Sec. II, we take $\alpha_1^{-1}(m_Z) = 59.02$, $\alpha_2^{-1}(m_Z) = 29.58$ and $\alpha_3^{-1}(m_Z) = 8.36$ [18]. Defining the parameter $t = \ln(\mu/m_Z)$, we evaluate the RGE's between $t = 0$ and $t_* = \ln(M_*/m_Z) \approx 37.8$, ignoring threshold corrections at the weak scale. We note that our requirement that the couplings remain bounded everywhere in this interval may be overly conservative, since (as theories of TeV-scale gravity have illustrated) the cut off at which gravitational physics becomes relevant may in fact be substantially smaller than M_* .

We are also now equipped to determine the vacuum stability of the model at each point in parameter space. In the standard model, one runs the Higgs quartic coupling to higher renormalization scales and determines whether there are points where the coupling becomes negative. This result implies that the effective potential becomes unbounded from below. In two-Higgs doublet models, the standard approach is also to run the couplings of the tree-level potential, and to check that the tree-level stability conditions remain satisfied.

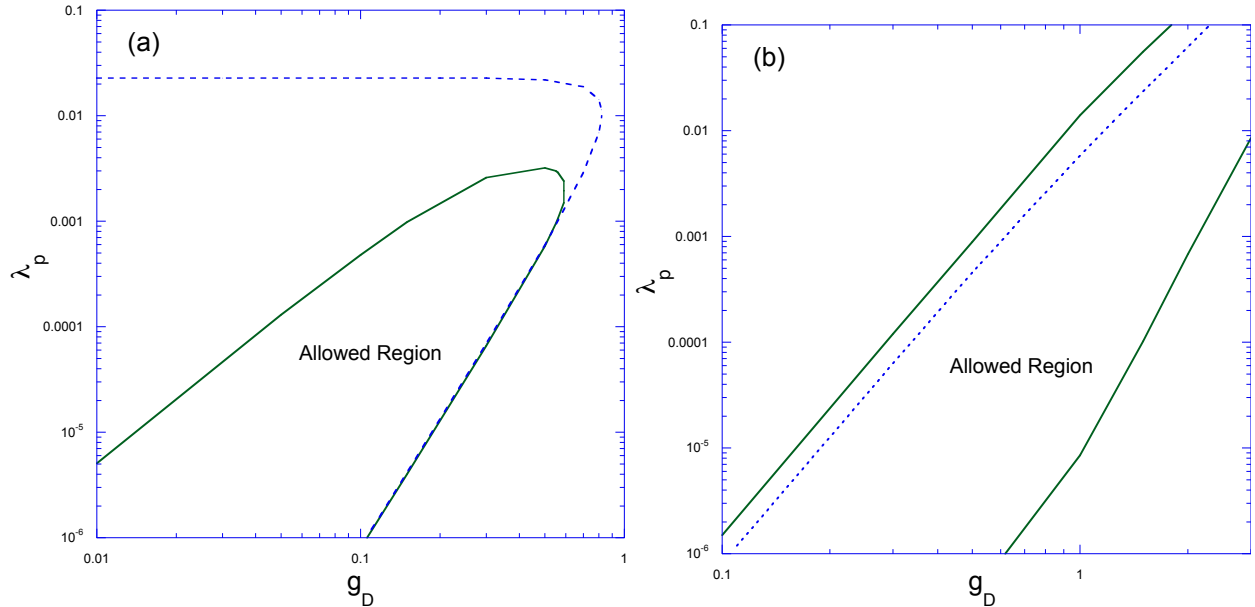


FIG. 1: Regions of the g_D - λ_p plane that are consistent with the perturbativity and vacuum stability constraints discussed in the text. In (a), $m_\eta < m_h$, while in (b), $m_\eta > m_h$. The regions above and to the right of the dashed line in (a) and above the dashed line in (b) correspond to $\sin^2 \theta > 0.1$.

The justification for this procedure is discussed in some detail in Ref. [19]. Applying this approach to the present model, we require at large renormalization scales that Eq. (2.3) remain satisfied. As discussed in Ref. [20], we do not expect these conditions to be satisfied at small scales, since we know that at small t the tree-level potential is *not* stable; the one-loop corrections are necessary ingredients for obtaining vacuum stability in this region. Given a choice of the two free parameters, the values and signs of all the remaining couplings are determined. Hence, our scan over parameter space will include all possible values of the electroweak-scale couplings that are phenomenologically viable. We then require that Eq. (2.3) remain satisfied over some range $t_0 < t < t_*$ with t_0 sufficiently larger than zero to eliminate cases in which the potential turns over and becomes unbounded from below at large field values. For definiteness, we take $t_0 = 5$ in computing our numerical results; our conclusions are not sensitive to the precise value of t_0 . The allowed regions that remain after the constraints of perturbativity and vacuum stability are imposed are shown in Fig. 1. There is no simple qualitative explanation for the shapes of these regions. Eqs. (2.7) and (2.8) as well as the RGEs are nonlinear; at some points in parameter space, λ_H reaches a Landau pole before M_* , while at nearby points one of the other couplings is first to become unacceptably large or leads to a violation of a stability condition. Note that we do not extend these plots to smaller values of g_D , since we will find that relatively large values of the couplings are required to obtain the desired dark vector annihilation cross section. This will be discussed in the next section.

The remaining issue we wish to address in this section is Higgs boson physics. The fact that the scalar mass eigenstates are mixtures of σ_0 and φ , where σ_0 would otherwise correspond to the standard model Higgs field, suggests that the model could lead to observable deviations of Higgs properties away from their standard model expectations. The production cross section times branching fractions of the Higgs-like eigenstate are proportional to $\cos^2 \theta$ times their standard model values. Current LHC bounds imply that this proportionality factor can be no smaller than ≈ 0.7 [21]. Moreover, if the mixing is large, then the otherwise “dark” Higgs η would develop large enough couplings to the visible sector to be detected in Higgs boson searches at the LHC¹. In this case, the partial widths to standard model quarks, leptons and gauge bosons are $\sin^2 \theta$ times the value for a standard model Higgs. Ignoring

¹ For an interesting exception to this statement, see Ref. [23]

possible decay to two standard model Higgs, one would expect that the branching fractions for the η state to be the same as a standard model Higgs boson, but the production cross section suppressed by a factor of $\sin^2 \theta$. LHC heavy Higgs search bounds can all be evaded for $\sin^2 \theta \lesssim 0.1$ [22]. Hence, we show in Fig. 1 the regions in which $\sin^2 \theta$ exceeds this value. The true constraint is actually weaker (since the LHC bound is not as restrictive as 0.1 for all scalar boson masses) but the distinction is not important here since the difference this produces in the allowed parameter region of Fig. 1 is relatively small.

IV. VECTOR DARK MATTER

Let us now consider the $SU(2)_D$ gauge boson interactions in the model,

$$\mathcal{L}_{SU(2)_D} = -\frac{1}{4} (F_{\mu\nu}^a)^2 + |D_\mu \Phi|^2, \quad (4.1)$$

where $F_{\mu\nu}^a = \partial_\mu A_\nu^a - \partial_\nu A_\mu^a + g_D \epsilon^{abc} A_\mu^b A_\nu^c$ and $D_\mu = \partial_\mu - ig_D T^a A_\mu^a$. The second term of (4.1) contains interactions between φ and the A^a gauge fields:

$$\mathcal{L}_{SU(2)_D} = -\frac{1}{4} (F_{\mu\nu}^a)^2 + \frac{1}{2} |\partial_\mu \varphi|^2 + \frac{1}{8} g_D^2 A_\mu^a A^{a\mu} (v_D + \varphi)^2. \quad (4.2)$$

Eq. (4.2) exhibits a non-anomalous $SO(3)$ symmetry under which the three gauge bosons transform as a triplet; the other particles in the model are singlets under this symmetry. As pointed out in Refs. [16], this $SO(3)$ symmetry is responsible for preserving the stability of the dark gauge boson multiplet. If higher-dimension operators were present, this symmetry could be broken, leading to a decaying dark matter scenario; this possibility is discussed in the second paper of Ref. [16]. Such dimensionful operators cannot be introduced here due to the assumption of classical scale invariance. After re-expressing φ and σ_0 in terms of the mass eigenstates h and η , one may isolate the leading diagrams that are responsible for dark gauge boson annihilation; in the case of small mixing angle θ (which is the relevant limit, given the results of the previous section), one obtains a reasonable approximation by considering the diagrams shown in Fig. 2. These diagrams are relevant provided that the second Higgs field η remains in thermal equilibrium with the ordinary standard model particle content up to the point at which dark gauge boson freeze-out occurs. We will come back to this point later. For the purposes of our relic density estimate, we omit diagrams that change dark matter number by only one unit, i.e., $AA \rightarrow A\eta$, the same assumption

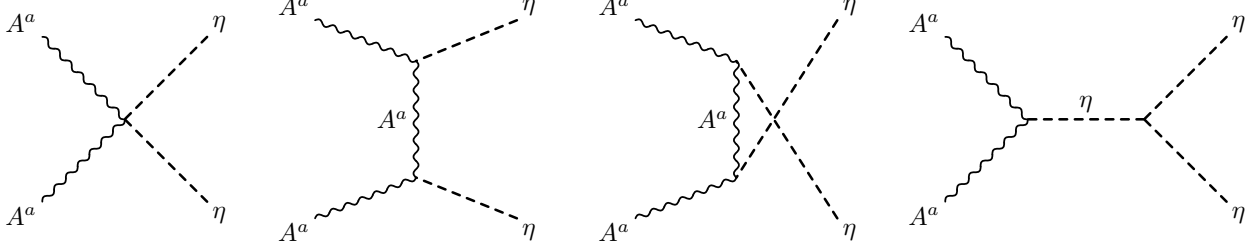


FIG. 2: Dark gauge boson annihilation diagrams included in the relic density estimate presented in the text.

made in the first paper of Ref. [16]. For the parameter region in which we obtain the desired $\Omega_D h^2$, the Higgs portal coupling $\lambda_P \gtrsim 0.001$; in the second paper of Ref. [16], it was found for similar Higgs portal couplings that the omitted diagrams did not substantially affect the relic density estimate; we leave their inclusion, as well as sub-leading diagrams that change dark matter number by two units, for a more detailed analysis in future work.

We find that the thermally averaged annihilation cross section times relative velocity that follows from Fig. 2 is

$$\begin{aligned}
 \langle \sigma_{\text{ann}} v \rangle = & \frac{g_D^4 \cos^4 \theta}{192 \pi m_A^2} \sqrt{1 - \frac{m_\eta^2}{m_A^2}} \left[\left(\frac{3}{2} \frac{\lambda \langle \varphi \rangle^2 \cos^2 \theta}{(4m_A^2 - m_\eta^2)} + \frac{1}{2} \right)^2 \right. \\
 & - \frac{4}{3} \left(\frac{m_A^2}{m_\eta^2 - 2m_A^2} \right)^2 \left(8 - 6 \frac{m_\eta^2}{m_A^2} + \frac{m_\eta^4}{m_A^4} \right) \left(\frac{3}{2} \frac{\lambda \langle \varphi \rangle^2 \cos^2 \theta}{(4m_A^2 - m_\eta^2)} + \frac{1}{2} \right) \\
 & \left. + \frac{4}{3} \left(\frac{m_A^2}{m_\eta^2 - 2m_A^2} \right)^2 \left(6 - 4 \frac{m_\eta^2}{m_A^2} + \frac{m_\eta^4}{m_A^4} \right) \right]. \quad (4.3)
 \end{aligned}$$

From this result, the freeze-out temperature and relic density are numerically calculated. With $x \equiv m_A/T$, we find numerically that the freeze-out temperature is typically in the range $x_F \approx 26 - 27$. The relic density is given by

$$\Omega_D h^2 \approx 3 \cdot \frac{(1.07 \times 10^9 \text{ GeV}^{-1}) x_F}{\sqrt{g_*(x_F)} M_{Pl} \langle \sigma v \rangle_F} \quad (4.4)$$

where the factor of 3 takes into account the size of the $\text{SU}(2)_D$ gauge multiplet. As a point of reference, we note that if all species are dynamical and in equilibrium, one would find $g_* = 122$; we take into account the temperature dependence of g_* in our numerical analysis.

The region in parameter space where $0.1048 < \Omega_D h^2 < 0.1228$, the $\pm 2\sigma$ band for the WMAP result 0.1138 ± 0.0045 [24], is shown in Fig. 3, together with our previous constraints.

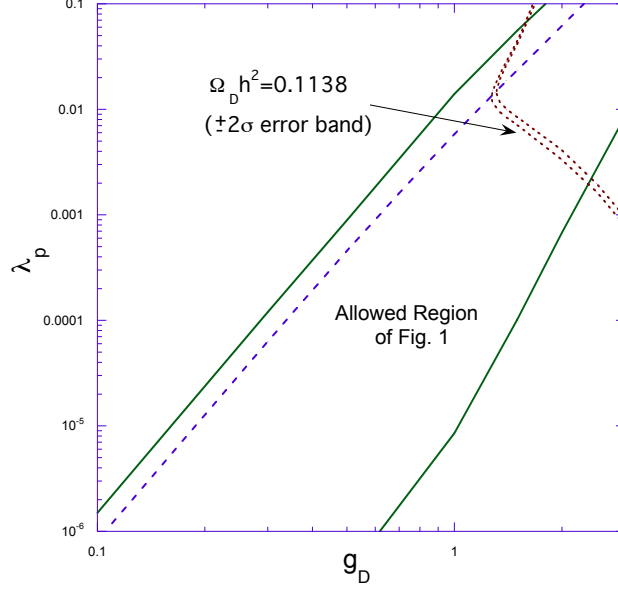


FIG. 3: Band where the dark gauge multiplet provides the dark matter relic density within $\pm 2\sigma$ experimental uncertainty.

In order to accommodate the observed relic density, the annihilation cross section must be sufficiently large, which in turn requires larger values of g_D and λ_p than allowed if $m_\eta < m_h$. Hence, our relic density results shown relative to the allowed parameter region of Fig. 1b.

We note that for all the allowed points in this band, the η remains in thermal equilibrium with the standard model particle bath at the time that the dark matter freezes out. The relevant constraint (following from decay and inverse decay) is $\Gamma_\eta > H(x_F)$, where Γ_η is the η decay width and H is the Hubble parameter [17]; we find that this inequality is satisfied by many orders of magnitude for allowed points in the $\Omega_D h^2$ band. Moreover, we find that the two-into-two process $\eta\eta \rightarrow hh$ is sufficient for maintaining η equilibrium by itself, for all points in the $\Omega_D h^2$ band that are also within the previously allowed region.

Finally, we check the compatibility of our results with current dark matter direct detection bounds. The dark matter-nucleon elastic scattering cross section is given by

$$\sigma(NA \rightarrow NA) = \frac{1}{64\pi} f^2 g_D^4 \sin^2 2\theta \frac{m_N^2 \langle \varphi \rangle^2 (m_\eta^2 - m_h^2)^2}{m_A^2 \langle \sigma \rangle^2 m_\eta^4 m_h^4} \left(\frac{m_N m_A}{m_N + m_A} \right)^2 \quad (4.5)$$

where m_N is the nucleon mass and f parameterizes the Higgs-nucleon coupling. In Table I, we provide more detailed information on a sampling of points within the $\Omega_D h^2$ allowed band of Fig. 3, including the direct detection cross section. The table displays results for $f = 0.3$; for different choices of f , the results can be scaled according to Eq. (4.5). All the points

g_D	$\lambda_p (\times 10^{-3})$	$\langle \varphi \rangle$ (GeV)	m_A (GeV)	m_η (GeV)	$\sin \theta$	$\sigma(AN) (\times 10^{-45} \text{cm}^2)$
1.4	9.127	1410	987	235	0.0802	1.279
1.5	7.689	1531	1148	292	0.0417	0.5176
2.0	3.609	2228	2228	752	0.0036	0.00972
2.5	1.795	3158	3947	1666	0.0005	0.00031
3.0	0.8606	4561	6841	3465	0.00008	0.00001

TABLE I: Sample points with $\Omega_D h^2 = 0.1138$, the central WMAP value [24] used in Fig. 3. All points shown have an elastic scattering cross section $\sigma(AN)$ below the current Xenon100 direct detection bounds [25].

shown are consistent with the bounds from the Xenon100 experiment [25]. We find the same to be true for all points in the $\Omega_D h^2$ allowed band above $g_D \approx 1.23$.

It is now easier to see why this model can be categorized as a secluded dark matter scenario [17]. The dark matter annihilates to an unstable mediator particle, η , at a rate controlled primarily by the coupling g_D . On the other hand, the direct detection cross section, Eq. (4.5), can be made small independently, by choosing λ_p values at fixed g_D that produce small $\sin^2 2\theta$. Table I indicates this behavior as one moves along the $\Omega_d h^2$ band toward the right side of Fig. 3.

V. CONCLUSIONS

We have investigated an extension of the standard model that is classically scale-invariant and in which the electroweak scale arises via the Coleman-Weinberg mechanism [13]. Like similar models involving new Abelian gauge groups [8], our non-Abelian model communicates the dimensional transmutation that originates in a dark sector to standard model particles via the Higgs portal. We have shown that there are regions of the model parameter space in which the theory maintains vacuum stability and perturbativity between the electroweak and the Planck scales, and in which the modifications to the Higgs sector would not yet have been discerned at the LHC. We have also shown that the particular gauge extension we discuss provides a dark matter candidate, a multiplet of stable vector bosons which behaves in accord with secluded dark matter scenarios [17] that have been discussed in the

literature.

We note that modifications of this model may also be of interest. For example, if one wanted a similar non-Abelian scenario with fermionic rather than vector dark matter, then one could introduce dark fermions that obtain masses only via spontaneous $SU(2)_D$ breaking (so as not to introduce any new fundamental mass scale) and provide a decay channel for the dark gauge boson multiplet. In such a scenario, a new fermion could be a potential dark matter matter candidate. And as indicated earlier, one might entertain weakening the constraints we've considered by taking the gravitational cut off of the theory to be lower than the conventional Planck scale. Many other variations of the model and the analysis are conceivable.

In light of the current LHC data, the origin of the electroweak scale and the nature of the hierarchy problem merit an exploration of the widest range of theoretical possibilities, including the classically scale-invariant scenarios that have re-emerged as a possibility in the recent literature [8] and motivate the present work. In a few years, the LHC may provide more definitive guidance on whether the one of the more popular theoretical proposals or a less expected paradigm is relevant in describing physics at the TeV scale.

Note Added: After our manuscript was made public, we learned of work in another recent preprint that also considers an $SU(2)$ vector dark matter model in a scale-invariant context: see Ref. [26].

Acknowledgments

This work was supported by the NSF under Grant PHY-1068008. In addition, C.D.C. thanks Joseph J. Plumeri II for his generous support.

-
- [1] See, for example, H. Baer and X. Tata, “Weak scale supersymmetry: From superfields to scattering events,” Cambridge, UK: Univ. Pr. (2006) 537 pp.
 - [2] N. Arkani-Hamed, A. G. Cohen, E. Katz, A. E. Nelson, T. Gregoire and J. G. Wacker, JHEP **0208**, 021 (2002) [hep-ph/0206020].

- [3] B. Grinstein, D. O’Connell and M. B. Wise, Phys. Rev. D **77**, 025012 (2008) [arXiv:0704.1845 [hep-ph]].
- [4] See, for example, the ATLAS Collaboration summary plots at:
<https://twiki.cern.ch/twiki/bin/view/AtlasPublic/CombinedSummaryPlots>
- [5] W. A. Bardeen, FERMILAB-CONF-95-391-T.
- [6] R. Hempfling, Phys. Lett. B **379**, 153 (1996) [hep-ph/9604278]; W. -F. Chang, J. N. Ng and J. M. S. Wu, Phys. Rev. D **75**, 115016 (2007) [hep-ph/0701254 [HEP-PH]]; R. Foot, A. Kobakhidze, K. .L. McDonald and R. .R. Volkas, Phys. Rev. D **76**, 075014 (2007) [arXiv:0706.1829 [hep-ph]]; Phys. Rev. D **77**, 035006 (2008) [arXiv:0709.2750 [hep-ph]]; T. Hambye and M. H. G. Tytgat, Phys. Lett. B **659**, 651 (2008) [arXiv:0707.0633 [hep-ph]]; S. Iso, N. Okada and Y. Orikasa, Phys. Lett. B **676**, 81 (2009) [arXiv:0902.4050 [hep-ph]]; M. Holthausen, M. Lindner and M. A. Schmidt, Phys. Rev. D **82**, 055002 (2010) [arXiv:0911.0710 [hep-ph]]; R. Foot, A. Kobakhidze and R. R. Volkas, Phys. Rev. D **82**, 035005 (2010) [arXiv:1006.0131 [hep-ph]]; L. Alexander-Nunneley and A. Pilaftsis, JHEP **1009**, 021 (2010) [arXiv:1006.5916 [hep-ph]]; G. Marques Tavares, M. Schmaltz and W. Skiba, arXiv:1308.0025 [hep-ph]; A. Farzinia, H. -J. He and J. Ren, arXiv:1308.0295 [hep-ph].
- [7] K. A. Meissner and H. Nicolai, Phys. Lett. B **648**, 312 (2007) [hep-th/0612165]; Phys. Lett. B **660**, 260 (2008) [arXiv:0710.2840 [hep-th]].
- [8] S. Iso and Y. Orikasa, PTEP **2013**, 023B08 (2013) [arXiv:1210.2848 [hep-ph]]; C. Englert, J. Jaeckel, V. V. Khoze and M. Spannowsky, JHEP **1304**, 060 (2013) [arXiv:1301.4224 [hep-ph]].
- [9] M. Farina, D. Pappadopulo and A. Strumia, arXiv:1303.7244 [hep-ph].
- [10] M. Heikinheimo, A. Racioppi, M. Raidal, C. Spethmann and K. Tuominen, arXiv:1305.4182 [hep-ph].
- [11] T. Hur and P. Ko, Phys. Rev. Lett. **106**, 141802 (2011) [arXiv:1103.2571 [hep-ph]]; M. Heikinheimo, A. Racioppi, M. Raidal, C. Spethmann and K. Tuominen, arXiv:1304.7006 [hep-ph].
- [12] C. D. Carone and H. Georgi, Phys. Rev. D **49**, 1427 (1994) [hep-ph/9308205].
- [13] S. R. Coleman and E. J. Weinberg, Phys. Rev. D **7**, 1888 (1973).
- [14] J. D. Lykken, “Higgs without SUSY,” talk presented at *The first three years of the LHC*, Mainz, March 18-22, 2013.
- [15] G. ’t Hooft, NATO Adv. Study Inst. Ser. B Phys. **59**, 135 (1980).

- [16] T. Hambye, JHEP **0901**, 028 (2009) [arXiv:0811.0172 [hep-ph]]; C. Arina, T. Hambye, A. Ibarra and C. Weniger, JCAP **1003**, 024 (2010) [arXiv:0912.4496 [hep-ph]].
- [17] M. Pospelov, A. Ritz and M. B. Voloshin, Phys. Lett. B **662**, 53 (2008) [arXiv:0711.4866 [hep-ph]].
- [18] J. Beringer *et al.* [Particle Data Group Collaboration], Phys. Rev. D **86**, 010001 (2012).
- [19] M. Sher, Phys. Rept. **179**, 273 (1989).
- [20] G. Kreyerhoff and R. Rodenberg, Phys. Lett. B **226**, 323 (1989).
- [21] J. R. Espinosa, C. Grojean, M. Muhlleitner and M. Trott, JHEP **1212**, 045 (2012) [arXiv:1207.1717 [hep-ph]]; P. P. Giardino, K. Kannike, M. Raidal and A. Strumia, Phys. Lett. B **718**, 469 (2012) [arXiv:1207.1347 [hep-ph]].
- [22] S. Chatrchyan *et al.* [CMS Collaboration], Eur. Phys. J. C **73**, 2469 (2013) [arXiv:1304.0213 [hep-ex]].
- [23] M. Heikinheimo, A. Racioppi, M. Raidal and C. Spethmann, arXiv:1307.7146 [hep-ph].
- [24] G. Hinshaw *et al.* [WMAP Collaboration], arXiv:1212.5226 [astro-ph.CO].
- [25] E. Aprile *et al.* [XENON100 Collaboration], Phys. Rev. Lett. **109**, 181301 (2012) [arXiv:1207.5988 [astro-ph.CO]].
- [26] T. Hambye and A. Strumia, arXiv:1306.2329 [hep-ph].